# Fabrication of planar photonic crystals in a chalcogenide glass using a focused ion beam

**Darren Freeman, Steve Madden, and Barry Luther-Davies**

*CUDOS, Laser Physics Centre, Research School of Physical Sciences and Engineering*
*The Australian National University, Canberra, ACT 0200, Australia*
*dfreeman@ieee.org*

**Abstract:** Free-standing "AMTIR-1" ($Ge_{33}As_{12}Se_{55}$) chalcogenide glass films have been patterned using a focused ion beam (FIB) to create two-dimensional photonic crystal membranes. The triangular lattices were selected for a photonic bandgap relevant to fiber telecommunications. Optical measurements of transmission spectra as a function of incident angle showed clear signs of Fano resonances, indicating that the structures had strongly modified guided modes.

©2005 Optical Society of America

**OCIS codes:** (220.4000) Microstructure fabrication; (160.4330) Nonlinear optical materials; (350.3850) Materials processing

## References and links

1. W. Bogaerts, P. Bienstman, D. Taillaert, R. Baets, and D. De Zutter, "Out-of-plane scattering in photonic crystal slabs," IEEE Phot. Tech. Lett. **13**, 565-567 (2001).
2. Y. Tanaka, T. Asano, Y. Akahane, B.-S. Song, and S. Noda, "Theoretical investigation of a two-dimensional photonic crystal slab with truncated cone air holes," Appl. Phys. Lett. **82**, 1661-1663 (2003).
3. A. Zakery, Y. Ruan, A. V. Rode, M. Samoc, and B. Luther-Davies, "Low-loss waveguides in ultrafast laser-deposited $As_2S_3$ chalcogenide films," J. Opt. Soc. Am. B **20**, 1844-1852 (2003).
4. Y. Ruan, W. Li, R. Jarvis, N. Madsen, A. Rode, and B. Luther-Davies, "Fabrication and characterization of low loss rib chalcogenide waveguides made by dry etching," Opt. Express **12**, 5140-5145 (2004), http://www.opticsexpress.org/abstract.cfm?URI=OPEX-12-21-5140.
5. V. N. Astratov, A. M. Adawi, M. S. Skolnick, V. K. Tikhomirov, V. Lyubin, D. G. Lidzey, M. Ariu, and A. L. Reynolds, "Opal photonic crystals infiltrated with chalcogenide glasses," Appl. Phys. Lett. **78**, 4094-4096 (2001).
6. B. H. Juárez, S. Rubio, J. Sánchez-Dehesa, and C. López, "Antimony trisulfide inverted opals: growth, characterization, and photonic properties," Adv. Mat. **14**, 1486-1490 (2002).
7. H.-Y. Lee and T. Yao, "Wet-etching selectivity of Ag-photodoped AsGeSeS thin films and the fabrication of a planar corrugated one-dimensional photonic crystal by a holographic method," J. Vac. Sci. Tech. B **20**, 2017-2023 (2002).
8. A. Feigel, Z. Kotler, B. Sfez, A. Arsh, M. Klebanov, and V. Lyubin, "Chalcogenide glass-based three-dimensional photonic crystals," Appl. Phys. Lett. **77**, 3221-3223 (2000).
9. A. Feigel, M. Veinger, B. Sfez, A. Arsh, M. Klebanov, and V. Lyubin, "Three-dimensional simple cubic woodpile photonic crystals made from chalcogenide glasses," Appl. Phys. Lett. **83**, 4480-4482 (2003).
10. S. J. McNab, N. Moll, and Y. A. Vlasov, "Ultra-low loss photonic integrated circuit with membrane-type photonic crystal waveguides," Opt. Express **11**, 2927-2939 (2003), http://www.opticsexpress.org/abstract.cfm?URI=OPEX-11-22-2927.
11. L. Vogelaar, W. Nijdam, H. A. G. M. van Wolferen, R. M. de Ridder, F. B. Segerink, E. Flück, L. Kuipers, and N. F. van Hulst, "Large area photonic crystal slabs for visible light with waveguiding defect structures: fabrication with focused ion beam assisted laser interference lithography," Adv. Mat. **13**, 1551-1554 (2001).
12. G. Dale, R. M. Langford, P. J. S. Ewen, and C. M. Reeves, "Fabrication of photonic band gap structures in $As_{40}S_{60}$ by focused ion beam milling," J. Non-Cryst. Solids **266-269**, 913-918 (2000).
13. A. V. Rode, B. Luther-Davies and E. G. Gamaly, "Ultrafast ablation with high-pulse-rate lasers," Part II: experiments on laser deposition of amorphous carbon films, J. Appl. Phys. **85**, 4222-4230 (1999).
14. S. Fan and J. D. Joannopoulos, "Analysis of guided resonances in photonic crystal slabs," Phys. Rev. B **65**, 235112 (2002).

#6714 - $15.00 US Received 28 February 2005; revised 6 April 2005; accepted 6 April 2005
(C) 2005 OSA

15. V. Lousse, W. Suh, O. Kilic, S. Kim, O. Solgaard, and S. Fan, "Angular and polarization properties of a photonic crystal slab mirror," Opt. Express **12**, 1575-1582 (2004), http://www.opticsexpress.org/abstract.cfm?URI=OPEX-12-08-1575.
16. V. Lousse and J. P. Vigneron, "Use of Fano resonances for bistable optical transfer through photonic crystal films," Phys. Rev. B **69**, 155106 (2004).

## 1. Introduction

Photonic crystals (PhCs) are a relatively new class of optical structure, in which the propagation of light is controlled using a strong periodic modulation of the refractive index on a spatial scale much shorter than the free-space optical wavelength. With sufficiently high index contrast ($\Delta n \approx 1.5$), the modulation results in the appearance of gaps in the photonic bands, within which light cannot propagate. This phenomenon provides a new way to trap, control and manipulate light that appears to have significant potential for future optical technology. The introduction of a linear defect, for example a row of missing holes or rods, introduces guided modes that have no radiative modes to couple into, due to the band-gap of the surrounding lattice.

To make two-dimensional (2D) PhC devices at telecommunications wavelengths (1.3 or 1.55 μm), the modulation period is in the 300-600 nm range, depending on the refractive index, the thickness of the material and the shape of the unit cell. Typically the light is guided in the third dimension by total internal reflection (TIR) so an appropriate cladding material (e.g. air) is chosen with a lower refractive index than the PhC slab. To make a device it is necessary to accurately perforate the PhC slab (and sometimes the cladding) over tens or hundreds of periods and produce very smooth interfaces. Defect guiding is very sensitive to fabrication errors because of the possibility of coupling to the out-of-plane radiative modes. To mitigate this loss mechanism, the guided modes should lie below the *light-line*, meaning their effective index is higher than the cladding index and therefore they are not phase-matched to radiative modes. Nevertheless practical devices will always involve spatial Fourier components that radiate out of the plane, so fabrication quality is crucial [1].

PhC slabs should be symmetrical if the TE- and TM-like modes are to remain orthogonal. If this is not achieved and the lattice has only a partial (i.e. TE- or TM-only) bandgap, cross coupling can transfer power to the lossy mode, compromising device performance [2]. Symmetry in practice requires both vertical sidewalls and identical upper and lower claddings. Use of air both above and below the structure is favored because it maintains symmetry and helps to keep the defect modes below the light-line. Such a structure is known as a free-standing PhC membrane.

In this paper we present results on the preparation of 2D PhC lattices in 300 nm thick membranes of "AMTIR-1" chalcogenide glass ($Ge_{33}As_{12}Se_{55}$). Chalcogenide glasses are infrared transmitting materials containing the chalcogen elements S, Se or Te, compounded with such elements as As, Ag and Ge. Glasses can be formed over a wide range of compositions, allowing tuning of parameters such as their electronic band-edge and refractive index. The index is typically between 2.4 and 3.0, and the absorption losses are low over a wide range of wavelengths, between the electronic band-edge in the visible or near infrared, and the Restrahlen bands in the mid-infrared. We are particularly interested in their relatively large third-order optical nonlinearity (100-1000× that of silica) and low two-photon absorption which suggests that they might be used for all-optical ultra-fast switching at low powers in structures having tight optical confinement [3].

In order to explore the potential of these materials for planar photonics it is necessary to develop techniques for both the deposition of high quality films as well as nano-patterning to create complex photonic structures. Whilst we are also pursuing conventional approaches for device fabrication using contact printing and reactive-ion etching [4], we report here an alternative method using a focused ion beam (FIB). We demonstrate a free-standing

#6714 - $15.00 US Received 28 February 2005; revised 6 April 2005; accepted 6 April 2005
(C) 2005 OSA

chalcogenide glass PhC membrane fabricated by FIB milling and also report some preliminary optical characterization.

Previously chalcogenide glass photonic crystals have been produced using entirely different techniques. Self-assembled 3D synthetic opal structures were used as a template into which chalcogenide glasses were infiltrated using wet chemistry [5,6]. Additionally, 1D PhC reflectors [7] and 3D woodpile structures [8,9] have been produced using photolithographic processes combined with wet etching. However, to the best of our knowledge this is the first report of a 2D chalcogenide glass PhC with sufficiently small lattice period to operate at telecommunications wavelengths.

To date, most 2D PhC structures in other materials have been fabricated using electron-beam or photolithography combined with dry etching. Whilst these processes are well developed for silicon as a result of CMOS fabrication and research into silicon-on-insulator photonic devices [10], this is not the case for most other high index optical materials. FIB milling provides a simple single-step approach that provides rapid prototyping of PhC devices in new materials without the need to optimize the conditions for dry etching. It is worth noting, however, that a FIB could also be used to pattern a mask or a photo-resist prior to dry etching as a substitute for e-beam lithography. A FIB has also been used to add defects to a predefined PhC mask, made by optical interference lithography, and this led to higher throughput at the expense of design flexibility [11].

Redeposition of sputtered material is an impediment to FIB milling of narrow, deep, blind holes. This is a common problem that is often alleviated by using a reactive gas. A previous attempt at PhC fabrication was made in a plate of $As_2S_3$ chalcogenide glass by FIB milling with and without the assistance of $I_2$ gas [12]. The highest aspect ratio of 6:1 was achieved with gas assistance at low beam currents, $\leq$12 pA. The fastest milling was obtained at the maximum beam current of 70 pA and the time to mill a hole of 1 $\mu m^3$ was 91 s. This is an effective sputter yield of 0.15 $\mu m^3$/nC, limiting the practicality of milling sufficiently large structures to form a photonic crystal.

Redeposition was not found to be a serious problem when milling holes through a thin membrane in our work, where the required aspect ratio was only 1:1.

## 2. FIB system

Our FIB system consists of an Orsay Physics CANION 31Mplus FIB mounted to the specimen chamber of a JEOL JSM-6460LV scanning electron microscope (SEM). In this work the FIB produced a tightly focused beam of $Ga^+$ ions (rated at <20 nm minimum spot size) with an energy of 30 keV. The beam was deflected electronically over a field size of $\approx$110 μm by an external input in the form of X/Y analog signals that were digitally generated with a step size of 1.7 nm. We developed our own pattern generation system, driven by custom software, which translates design information composed of basic geometrical objects, into waveforms that scan the beam over the sample to mill the desired pattern.

## 3. Film preparation and milling

AMTIR-1 glass supplied by Amorphous Materials Inc. (Garland, Texas), was deposited using our ultra-fast pulsed laser deposition technique [3,13] onto Si wafers as films around 300 nm thick. It should be noted that energy-dispersive x-ray (EDX) analysis indicated that our films had the same stoichiometry as the bulk glass, but measurements using an SCI Filmtek 4000 metrology tool indicate a higher refractive index than the bulk, $\approx$2.7 vs. 2.54 at 1.55 μm. This is most likely due to differences in the bond structure.

To produce nanostructures we used vector scanning as opposed to raster scanning for two reasons. Firstly we have observed that the outcome of milling depends strongly upon the precise beam path and its timing. This arises from thermal effects due to local heating that significantly affects the mill rate. Secondly we anticipated that the lowest surface roughness would be obtained when the sidewalls were milled using a trajectory that was parallel to the

#6714 - $15.00 US Received 28 February 2005; revised 6 April 2005; accepted 6 April 2005
(C) 2005 OSA

wall of the remaining structure. To mill an arbitrary hole shape we therefore used a sequence of beam paths that were locally parallel and separated by an appropriate pitch (e.g. 50 nm). Together these filled the hole with the outermost path coinciding with the user-specified shape. The linear speed was constant along these paths. Whilst the estimated diameter of the focused Ga beam is ≈20 nm, the smallest feature we have been able to mill to date is ≈50 nm with the parameters used in this work.

## 4. Free-standing PhC slab

To create the free-standing PhC slab, a 300 nm film of AMTIR-1 was floated from the Si substrate onto a water surface, and then captured by a copper mesh transmission electron microscopy (TEM) grid and dried. An intermediate layer of detergent was used to facilitate the separation of the film from the substrate. This film forms an air-clad slab waveguide that is single-mode at 1550 nm. We selected a triangular lattice of 500 nm period containing 300 nm diameter holes, making this structure relevant to optical telecommunications. An ideal structure would have a band-gap for TE-like modes around 1550 nm.

Several PhC slabs were fabricated by FIB milling and examined using a Hitachi S-4500 field-emission SEM (FESEM). Figure 1 shows a micrograph of part of one of these – a 200×231 triangular lattice containing 46,315 holes. The holes were milled one at a time since we found with larger holes (such as 1 μm diameter) that a higher milling rate was obtained in this mode compared with the alternative where multiple exposures of the whole pattern were overlaid. We attribute this to thermal effects associated with localized heating and poor thermal conductivity of the film in vacuum. For this lattice the beam current was 85 pA and each hole received a 200 ms exposure consisting of 100 repetitions for each of 50, 100, and 150 nm radii sequentially to leave a polished hole. The linear speed was the same throughout the process at 942 μm/s. The total exposure was 9263 s (2 hours and 34 minutes). The mill rate was estimated to be 0.106 $\mu m^3$/s (6.36 $\mu m^3$/min) and the effective sputter yield 1.25 $\mu m^3$/nC, which is a lower bound because a significant dose of ions passed through the structure. The FIB accurately reproduced the required pattern over an area much larger than required for most devices, indicating that drift was not significant over time periods required to write device sized structures. 20×20 $\mu m^2$ patterns, for example, were written in a relatively short time of 6 minutes.

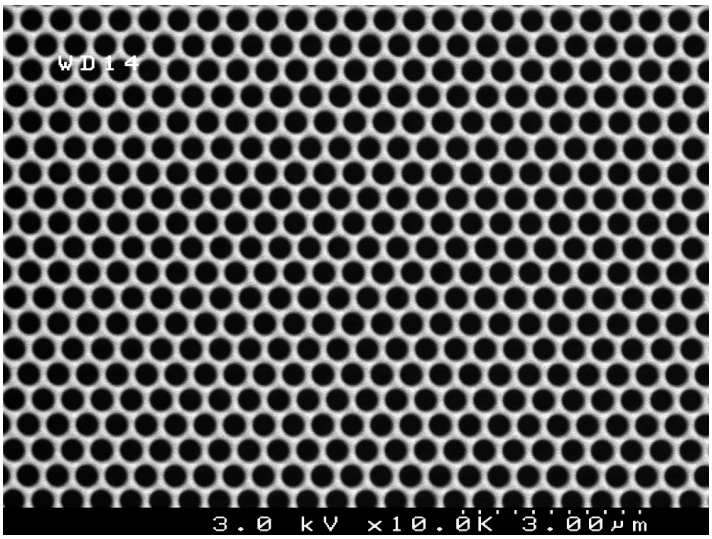


Fig. 1. 100×100 $\mu m^2$ free-standing photonic crystal membrane imaged at normal incidence to reveal long-range order. The holes were milled in horizontal rows.

#6714 - $15.00 US Received 28 February 2005; revised 6 April 2005; accepted 6 April 2005
(C) 2005 OSA

The highest resolution images failed to reveal any surface roughness over the bulk of the structure (see Fig. 2), despite the resolution of <3 nm as measured by inspecting the edge of a hole. It is possible that the roughness is not visible due to the depth of penetration of the 10 keV beam. From the images it was apparent that the holes were only slightly tapered along the majority of their length, with a change in slope at the top of the film where the sidewalls gently merge into the upper surface. Sculpting of the upper surface of the PhC, caused by the pedestal of the beam and possibly other effects, yielded rounded conical protrusions between the holes and a reduction in lattice symmetry. The walls between the holes have therefore been milled significantly. This surface modification might be acceptable or even useful for PhC use as-is, however it might also be eliminated by improving the milling algorithm or by over-coating the film with a removable, sacrificial layer.

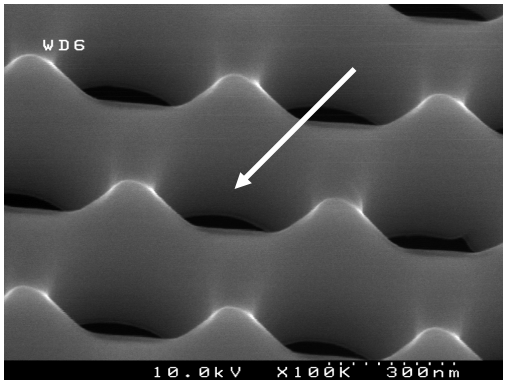


Fig. 2. High-resolution (<3 nm) close-up of the free-standing photonic crystal slab of Fig. 1, at 45°. The holes were milled sequentially in rows in the direction of the arrow. Successive rows were stacked from left to right.

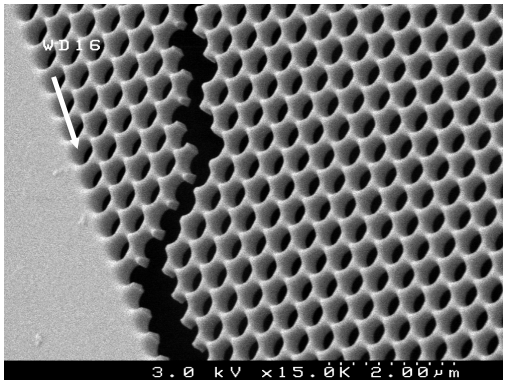


Fig. 3. A crack through the bottom of a 20×20 $\mu m^2$ structure fabricated on the same film as Fig. 1. The holes were milled sequentially in rows in the direction of the arrow. Successive rows were stacked from left to right.

The crack in Fig. 3 provides a cross-section along two lattice-vector orientations, allowing an observation of the sidewall profile that is rounded at the top, straight and roughly vertical along its length, and sharp at the bottom. From images taken at normal incidence we estimated the hole diameter to be 290 nm at the base, increasing to 360 nm at the rounded top.

The achievable positional accuracy of the FIB is believed to be at the nm level, with the lattice period being determined by the accuracy of the calibration performed in software. Accuracy in the radius of the holes is more difficult to specify since the beam width was not specifically taken into account, nor was the material behavior known *a priori*.

## 5. Optical test

To demonstrate the optical activity of the large structure of Fig. 1, we employed the guided resonance phenomenon [14] also known as “Fano” resonance. In principle, by taking transmission and reflection spectra as a function of incident angle on membrane PhC structures, it is possible to verify the band structure of the guided Bloch modes lying above the light-line. Essentially the incident beam is transmitted according to its Fabry-Pérot resonances, determined from an effective-index model of the perforated structure. There are also a number of narrow resonances that occur when the incident frequency and in-plane wave-vector couple to a guided resonance of the slab and subsequently leak out again as traveling waves. The spectral form of these resonances is roughly Lorentzian, with a line-width determined by more complex details of the Bloch mode. When the transmitted and reflected beams interfere with the leaking waves from the excited resonances, they can form very sharp spectral features swinging from nearly total reflection to total transmission, due to the $\pi$ phase shift associated with crossing the central frequency of the Lorentzian resonance.

#6714 - $15.00 US Received 28 February 2005; revised 6 April 2005; accepted 6 April 2005
(C) 2005 OSA

The measured transmission spectra for each outgoing linear polarization state, as a function of incident angle along the Γ-K direction of the lattice (along which the holes were milled one row at a time), were taken for a relatively flat region in the center of the large PhC structure. The incident light was provided by a mercury arc lamp and delivered via an SMF-28 fiber to the film. The transmitted light was lens-coupled into a multi-mode fiber and fed to an ANDO AQ6317B optical spectrum analyzer. A polarizer was placed on the collection side for convenience, but it should be noted that PhC mirrors do not always conserve the polarization state of the transmitted beam [15]. The distance between the output of the fiber and the film varied from <20 μm to 80 μm as the angle of incidence progressed from normal incidence to 60°. Due to diffraction from the fibre, the spot size was varying in the range 10-20 μm as the angle increased. It was not helpful to use a larger spot size for these measurements in spite of the large area of the PhC, because the film was not sufficiently flat.

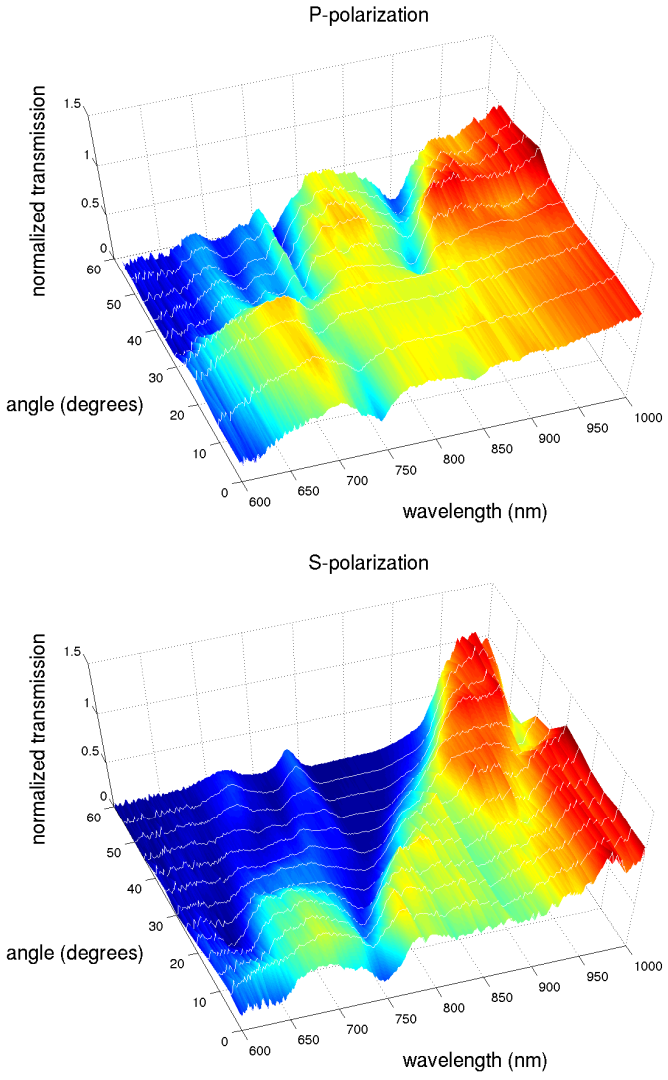


Fig. 4. Transmission spectra of a part of the 100×100 μm$^2$ photonic crystal slab, for both linear polarization states and as a function of angle of incidence along the Γ-K direction of the lattice.

#6714 - $15.00 US
Received 28 February 2005; revised 6 April 2005; accepted 6 April 2005
(C) 2005 OSA

The spectra are presented in the form of 2D linearly interpolated surfaces in Fig. 4. The two polarization states have completely different transmission spectra and there are spectral features that move smoothly in frequency as the angle is varied – a key characteristic of Fano resonances. We have omitted data for longer wavelengths because no features of interest were found, and below about 600 nm the material absorption was strong.

At present the sharpness of the features in Fig. 4 is limited by the relatively large divergence of the probe beam (≈5°) and residual curvature of the film. In addition, some alignment errors between input and output fibers led to imprecise normalization and uncertainties in the maximum transmission. Separate measurements using a 780 nm laser verified the abrupt transmission swing from nearly 0% to 100% as the angle was varied, for the feature observed with S-polarized incident light. While performing this measurement on a smaller structure, we created a short movie from images acquired using our alignment CCD camera as the angle was varied from normal incidence to 40°. Figure 5 shows the 20×20 μm$^2$ lattice and a representative frame from the movie, showing the effect of film curvature on the optical response. Clearly the flatness of the films needs improvement in further work.

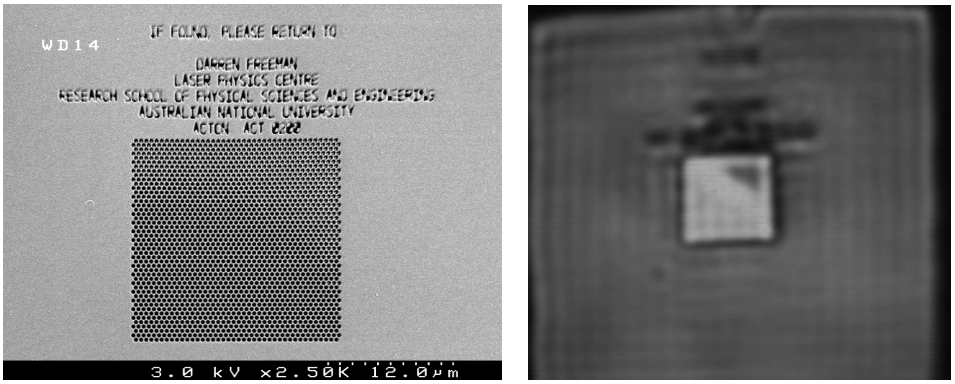


Fig. 5. (left) The 20×20 μm$^2$ lattice of Fig. 3 before it was damaged. (right, 625 kB) Movie of transmitted light at 780 nm as the sample was rotated through 0°-40°-0° in steps of 2°. The illustrated frame is at 10° and shows both enhanced and suppressed transmission.

## 6. Conclusion

We have demonstrated the use of a focused ion beam (FIB) to pattern free-standing chalcogenide glass films with a triangular lattice of 300 nm diameter holes and a 500 nm period. The FIB proved capable of accurately reproducing this lattice over areas as large as 100×100 μm$^2$ despite the relatively long writing time (>2 hours). The resulting patterns had very smooth sidewalls although sculpting of the upper surface was observed. We expect that this sculpting can be reduced by using more complex milling algorithms or sacrificial layers.

Measurements of the optical response of the lattice showed the clear presence of Fano resonances. In this case both the divergence of the probe beam and curvature of the free-standing films limited the quality of the data. When the sharpness of the spectral features is eventually improved, it may allow the demonstration of optical bistability in a chalcogenide PhC mirror [16].

In conclusion, we have demonstrated the ability to directly create nanoscale structures with smooth sidewalls in chalcogenide glass films using a FIB for direct milling. The one-step process is capable of rapid production of an almost unlimited range of complex patterns under software control, allowing rapid optimization of the structure to obtain particular optical functionality.

#6714 - $15.00 US Received 28 February 2005; revised 6 April 2005; accepted 6 April 2005
(C) 2005 OSA

**Acknowledgments**

Funding from the Australian Research Council (ARC) under its Centres of Excellence and Federation Fellow programs is gratefully acknowledged. The authors thank Andrei Rode and Nathan Madsen for depositing the chalcogenide glass films; Maryla Krolikowska for preparing the free-standing films; Christian Grillet (CUDOS, University of Sydney) for modeling and specification of the PhC design. Finally, we would like to thank Sally Stowe of the ANU Electron Microscopy Unit for use of the ANU FIB.

#6714 - $15.00 US Received 28 February 2005; revised 6 April 2005; accepted 6 April 2005
(C) 2005 OSA